Chemical weathering inferred from riverine water chemistry in the lower Xijiang basin, South China

Huiguo Sun [a,b,*], Jingtai Han [a], Dong Li [a], Shurong Zhang [b], Xixi Lu [b]

[a] Key Laboratory of Cenozoic Geology and Environment, Institute of Geology and Geophysics, Chinese Academy of Sciences, Beijing 100029, PR China
[b] Department of Geography, National University of Singapore, Singapore

ARTICLE INFO

ABSTRACT

Seasonal sampling was conducted on 13 sites involving the lower stem of the Xijiang river and its three tributaries to determine the spatial patterns of the riverine water chemistry and to quantify the chemical weathering rates of carbonate and silicate of the bedrock. Results indicate that the major ions in the Xijiang river system are dominated by Ca^{2+} and HCO_3^- with a higher concentration of total dissolved solids, characteristic of the drainages developed on typical carbonate regions. Obvious spatial variations of major ion concentrations are found at various spatial scales, which are dominantly controlled by the lithology particularly carbonate distribution in the region. The four selected rivers show similar seasonal variations in major ions, with lower concentrations during the rainy season. Runoff is the first important factor for controlling the weathering rate in the basin, although increasing temperature and duration of water–rock interaction could make positive contributions to the enhancement of chemical weathering. The chemical weathering rates range from 52.6 to 73.7 t/km²/yr within the lower Xijiang basin and carbonate weathering is over one order of magnitude higher than that of silicates. CO_2 consumption rate by rock weathering is 2.0×10^{11} mol/yr, of which more than 60% is contributed by carbonate weathering. The flux of CO_2 released to the atmosphere–ocean system by sulfuric acid-induced carbonate weathering is 1.1×10^5 mol/km²/yr, comparable with the CO_2 flux consumed by silicate weathering.

© 2010 Elsevier B.V. All rights reserved.

1. Introduction

Chemical weathering is a key part of earth surface processes that links geologic cycling of solid earth to the atmosphere and the ocean. Rock weathering consumes CO_2, mainly from atmospheric/soil origin, and produces aqueous HCO_3^- and CO_3^{2-}, then transport into the sea by rivers. On a geological time scale, the flux of CO_2 consumed by carbonate dissolution is balanced by the CO_2 flux released to the atmosphere by carbonate precipitation in the oceans, while chemical weathering of silicate rocks acts as a net sink for atmospheric CO_2. Consumption of atmospheric CO_2 plays an important role in effect on the long-term global air temperature (Caldeira, 1995; Gaillardet et al., 1999; Amiotte-Suchet et al., 2003). Inversely, the atmospheric temperature determines the chemical weathering rate and the associated consumption of the atmospheric CO_2. The temperature-dependence of weathering rate constitutes a negative feedback on atmospheric CO_2 (walker et al., 1981; Berner et al., 1983). The tendency and processes of global climate change are basically determined by the competing status of these factors. Hence, quantifying chemical weathering rates and clarifying the controlling factors are essential for understanding of Earth's climatic evolution.

As weathering products of terrestrial rocks are transported mainly by rivers, riverine water chemistry is often used for evaluation of chemical weathering rates in a catchment (Meybeck, 1987; Gaillardet et al., 1999; Mortatti and Probst, 2003). Rivers integrate various processes taking place in a basin, both natural and anthropogenic. A large number of studies have demonstrated that natural factors (lithology, temperature, runoff, relief and vegetation), particularly lithologic variations are dominant controls of water chemistry for both carbonate and silicate rivers (Gaillardet et al., 1999; Horowitz et al., 1999; Grasby and Hutcheon, 2000; Millot et al., 2002). However, the relative importance of these factors remains debatable. Some studies suggest that runoff controls the chemical weathering (Millot et al., 2002; Tipper et al., 2006), while others consider that temperature rather than runoff is more important (White and Blum, 1995; Dessert et al., 2001; Dalai et al., 2002). There are also studies emphasizing the factors such as physical erosion and water/rock contact time (Krishnaswami et al, 1999; Oliva et al., 2003; Hagedorn and Cartwright, 2009). With increasing influence of human activity, anthropogenic disturbance has been detected from water geochemistry in many rivers (Meybeck, 1998, 2003; Roy et al., 1999; Xu, 2004).

As a subtropical–tropical river featured with high temperature, plentiful rainfall, intense continental erosion and high population
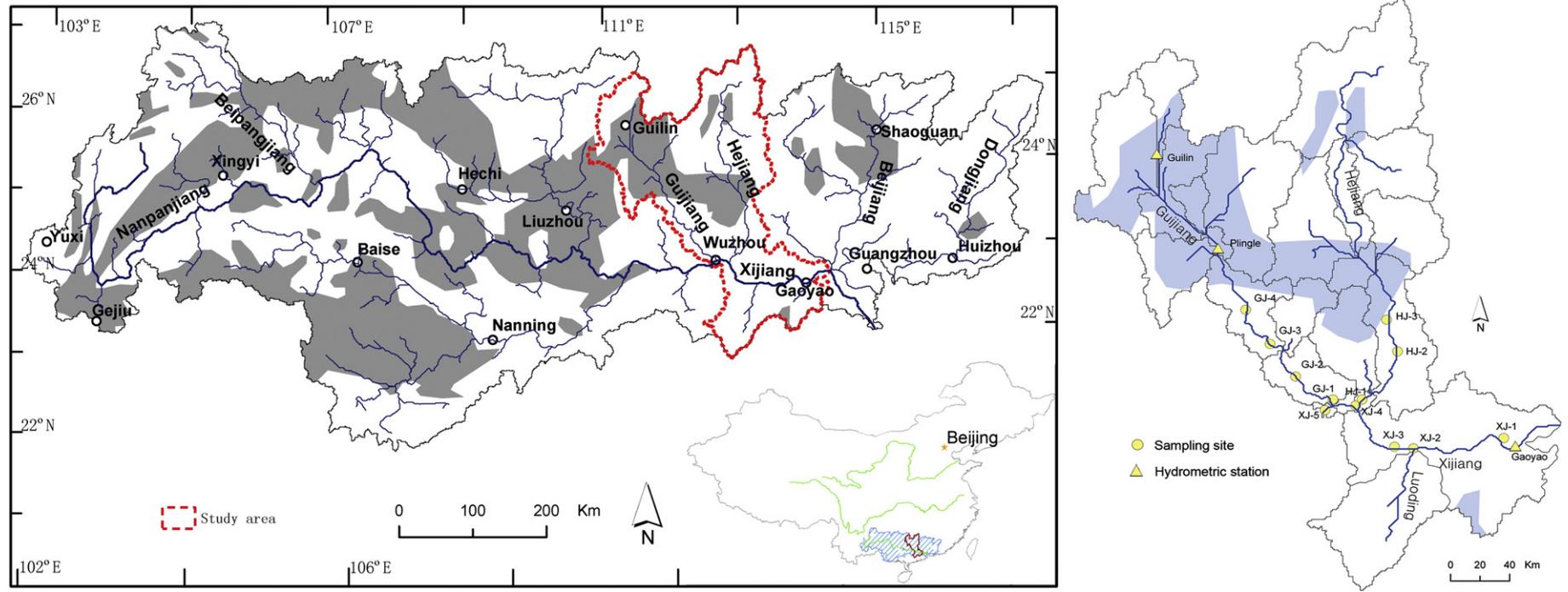
Fig. 1. The Xijiang river system and sampling localities. Shaded area is for carbonate bedrock.

Table 1
Characteristics of the tributary catchments of the Xijiang.

River	Area	Discharge	Channel slope	Carbonate	Silicate
	(km^2)	(km^3/yr)	(‰)	(km^2)	(km^2)
Xijiang[a]	351,535	218.1	0.86	149,402	202,133
Guijiang	18,210	17.1	0.43	9251	8959
Hejiang	11,590	8.01	0.58	2689	8901
Luoding	3164	2.68	0.87	253	2911

[a] Values for Xijiang represent the entire Xijiang basin, including the Guijiang, Hejiang and Luoding.

density, the Zhujiang (Pearl River) has drawn increasing attention in recent years. The major ion chemistry and flux of dissolved material in the Zhujiang have been generally characterized based on historic data in hydrology and water chemistry (Chen and He, 1999; Zhang et al., 2007). A number of studies focused on chemical wreathing and dissolved inorganic carbon (DIC) system of the Zhujiang basin (Xu and Liu, 2007; Li, et al., 2008; Gao et al., 2009; Zhang et al., 2009), largely addressing river geochemical signals. However, few studies paid attention to the spatial and temporal relations between these environmental factors, and the dominant factors for the chemical weathering in the basin remain to be explored.

In this study, the lower Xijiang and its three major tributaries were selected for detailed investigation. These tributaries developed in various basin sizes with markedly different proportions of carbonate/silicate in bedrock. By taking sampling simultaneously over the study area, we have a good chance to minimize the influence of the changes in runoff and temperature and focus on the effects of lithology on water chemistry. Through seasonal analysis, it allows us to identify the climatic sensitivity of the chemical weathering. This study attempts to (1) analyze seasonal and spatial patterns of major ion concentrations in the basin, (2) quantify carbonate and silicate weathering rates and the associated CO_2 consumption in each subbasin, and (3) evaluate the influences of the geologic and climatic factors on the weathering rates of carbonates and silicates.

2. Study area

The Zhujiang (Pearl river) is the second largest river in China in terms of annual discharge (336 km^3/yr) and the largest contributor for dissolved and solid materials to South China Sea (SCS) (PRWRC, 1991). It passes entirely through an evergreen forest area in the tropical–subtropical climate zone. The mean annual temperature and precipitation are 14~22 °C and 1200~2200 mm, respectively. Heavy rainfalls occur mainly in the period of June to August during which water discharge accounts for 50–60% of the annual amount.

The Zhujiang river system includes three principal branches, the Xijiang (West river), Beijiang (North river), and Dongjiang (East river) (Fig. 1). The Xijiang is the largest branch of the Zhujiang, accounting for 77.8% of total drainage area and 63.9% of the annual discharge of the entire Zhujiang. This study focused on the lower part of the Xijiang, where 3 major tributaries join the main channel of the Xijiang, namely Guijiang, Hejiang, and Luoding (Fig. 1). The Guijiang and Hejiang are two medium-size tributaries with a drainage area of 18,790 km^2 and 11,590 km^2, respectively. The Luoding is a small river with a drainage area of 3164 km^2. The monthly mean temperature is 13 °C in January and 28.5 °C in July in this region. The annual precipitation is 1629 mm. Based on historical database, the annual discharge is 17.1 km^3/yr in Guijiang, 8.0 km^3/yr in Hejiang and 2.7 km^3/yr in Luoding. The total flux of the Xijiang is up to 218.1 km^3/yr. As a typical monsoon region, the atmospheric (or water) temperature and precipitation (or discharge) in the Xijiang basin vary in a synchronous pattern; all high in summer and low in winter.

Carbonates are widely distributed in the Zhujiang Basin, especially in the headwater region of the Xijiang (Fig. 1) with typically

developed karst landscape, and covers about 39% of the total drainage area (PRWRC, 1991). The areas covered respectively with carbonate and silicate in each subbasin were calculated based on a map for rock type distribution. In the lower Xijiang, Quaternary fluvial sediments are abundant in the lower alluvial plain and the interior river valley plain. Additional characteristics of these sub-watersheds are listed in Table 1.

3. Sampling and laboratory analysis

Periodic sampling was conducted in the lower Xijiang basin, including the three major tributaries of Guijiang, Hejiang, Luoding, and the Xijiang stem (13 sampling sites; Fig. 1). The sampling sites were selected based on the spatial distributions of bedrock, vegetation, residential community location and confluent position of the tributaries. In each site, samples were taken from the middle depth of water column in the channel center. For seasonal variation analysis, samples were collected in April, May (yearly-normal flux), June (flood event), July (yearly-higher flux) and December (yearly-lower flux) (Fig. 2).

Temperature and pH values of the river water were measured in situ at each site. HCO_3^- concentration in the water was titrated with 0.01 M HCl within 24 h after sampling. Each sample was repeated for 2 or 3 times and the analytical error is less than 5%. Samples for major ion analysis were filtered by vacuum filtration through 47-mm Whatman GF/F filters (0.7 μm pore size) and stored in two 120 ml high-density polyethylene bottles at 4 °C until analysis. Samples for cation analysis were acidified (pH<2) with concentrated HNO_3. In the lab, major cations (K^+, Ca^{2+}, Na^+, Mg^{2+}) and dissolved Si were measured using an inductively coupled plasma optical emission spectrometer (ICP-OES). Major anions (Cl^-, SO_4^{2-}, NO_3^-) were measured by ion chromatography. Measurement of duplicate samples indicates the analytical error less than 3%.
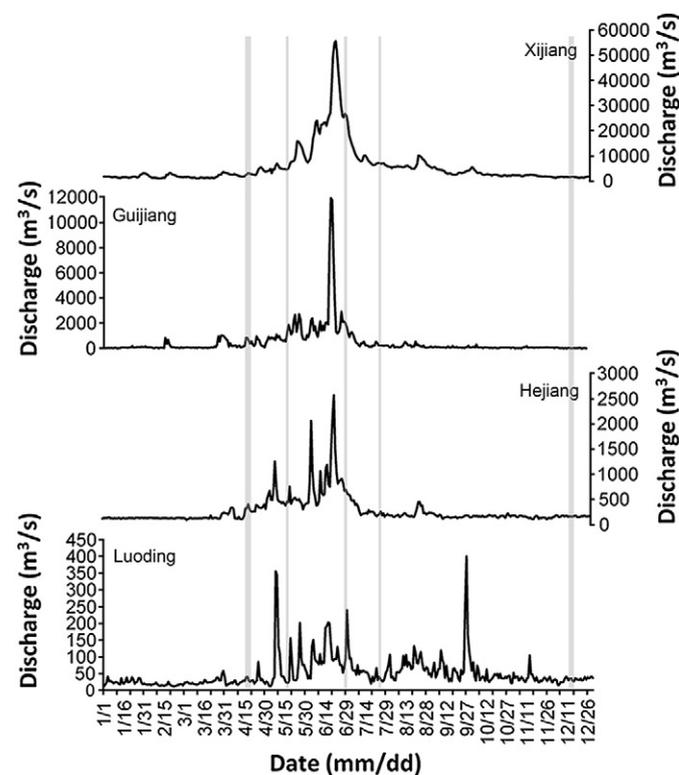
Fig. 2. Daily discharge of the Xijiang, Guijiang, Hejiang and Luoding in 2005. Data were monitored at hydrometric stations of Gaoyao, Majiang, Guhang and Guanliang (shown in Fig. 1). Sampling dates are marked by grey lines, and the width of the grey line represents sampling duration.
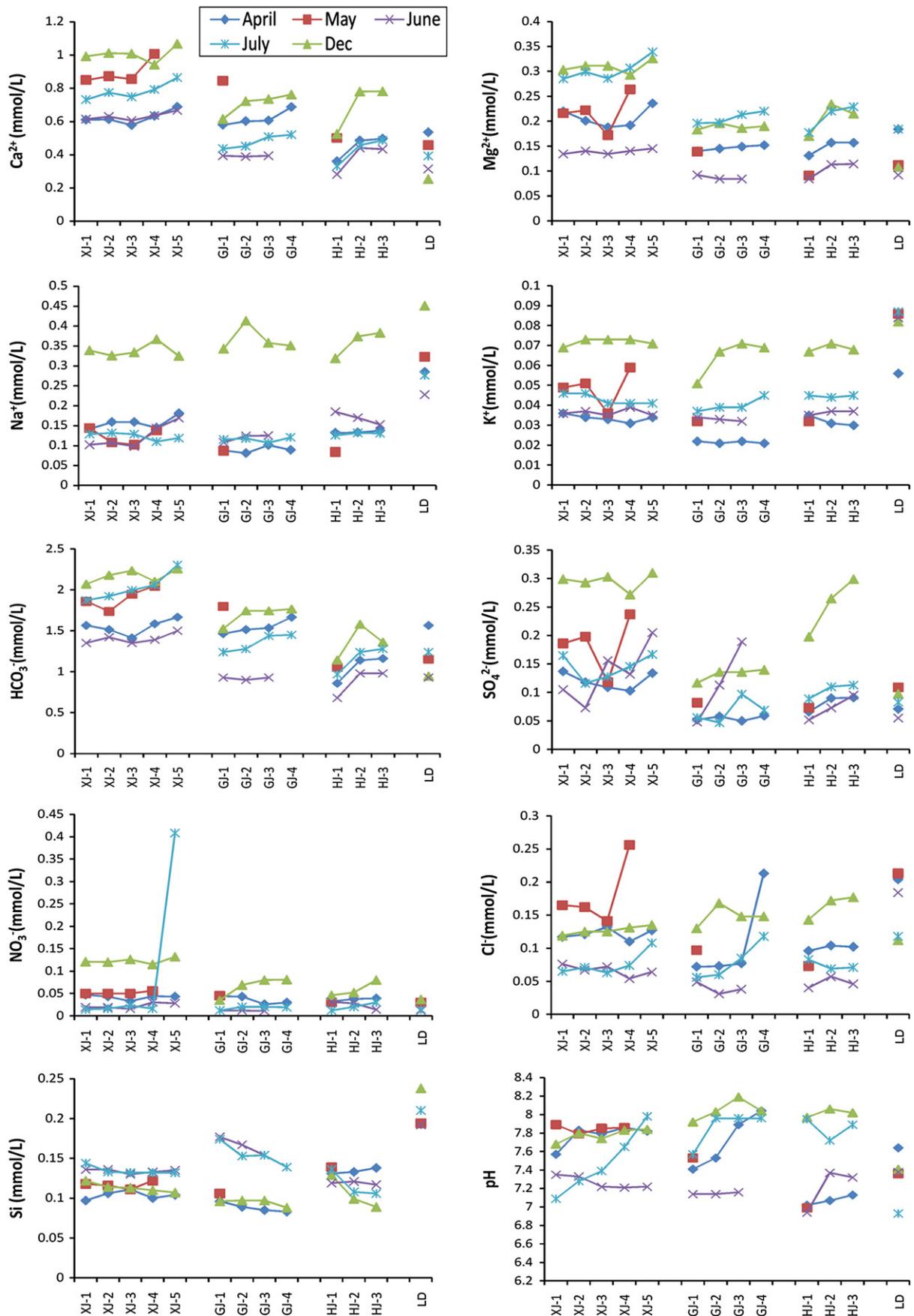
Fig. 3. Spatial and seasonal variations of major ions and pH value in the lower Xijiang basin.
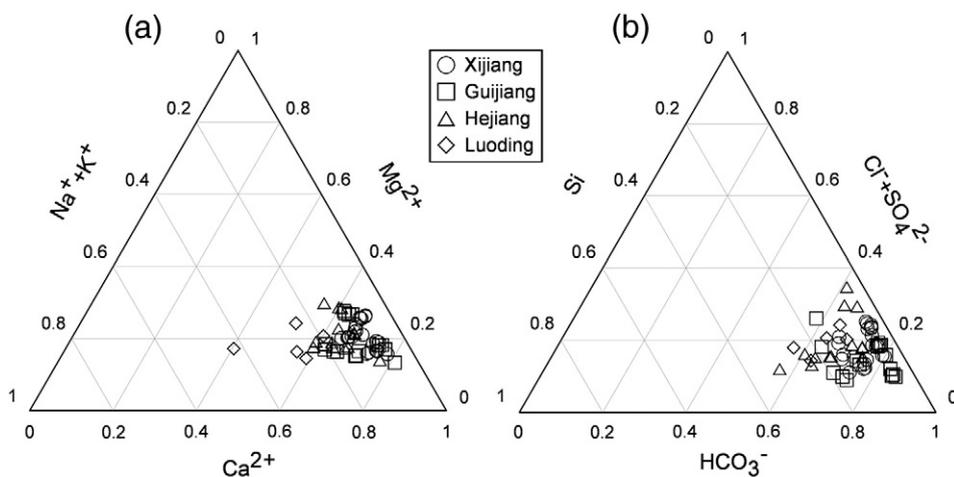
Fig. 4. Ternary plots showing relative abundances of cations (a) and anions (b) in the Xijiang river.

4. Results

4.1. General characteristics of major ions

pH value and major ion concentrations of the samples are shown in Table 2 and Fig. 3. The Xijiang river water is slightly alkaline with pH values between 6.93 and 8.19, and has a higher concentration of total dissolved solids $(TDS = Ca^{2+} + Mg^{2+} + Na^+ + K^+ + HCO_3^- + SO_4^{2-} + Cl^- + NO_3^- + SiO_2)$ with an average of 185 mg/L.

K^+ and Na^+ concentrations in the Xijiang river system range from 0.103 to 0.533 mmol/L, and should be most likely from silicate weathering because of little evaporites in the region. Ca^{2+} and Mg^{2+} commonly account for more than 60% of the total cations; about 83% (64% Ca^{2+}) in the Xijiang stem, 79% (62% Ca^{2+}) in the Guijiang, 74% (56% Ca^{2+}) in Hejiang and 57% (42% Ca^{2+}) in the Luoding. In general, Ca^{2+} and Mg^{2+} in river water can be derived from both carbonate and silicate weathering. Since carbonate has higher solubility, it produces more Ca^{2+} and Mg^{2+} than silicate under natural conditions. Therefore,
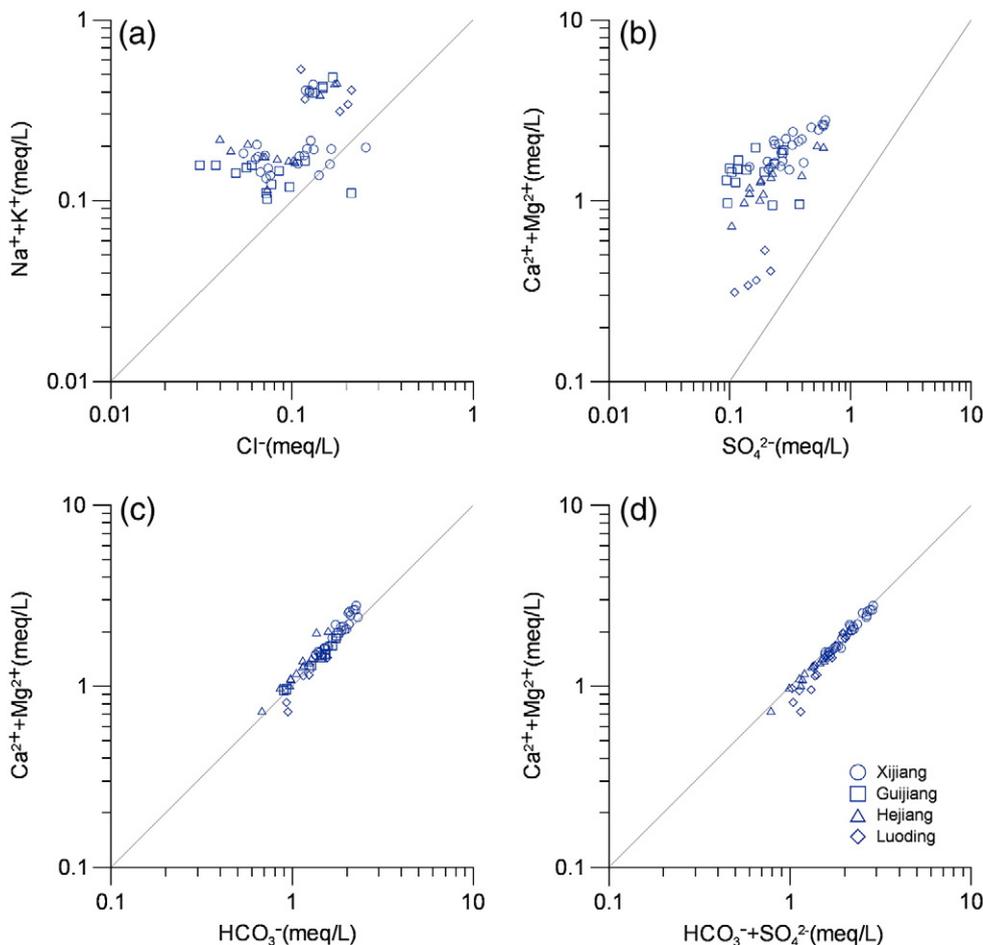
Fig. 5. Plots of (a) ($Na^+ K^+$) versus Cl^-, (b) ($Ca^{2+} + Mg^{2+}$) versus SO_4^{2-}, (c) ($Ca^{2+} + Mg^{2+}$) versus HCO_3^- and (d) ($Ca^{2+} + Mg^{2+}$) versus ($HCO_3^- + SO_4^{2-}$).

the wide distribution of carbonate in the Xijiang basin (except for the Luoding) is likely responsible for the observed higher concentrations of $Ca^{2+} + Mg^{2+}$.

HCO_3^- is the most abundant anion in the Xijiang river system, accounting for more than 80% of the total anions, particularly in the Xijiang stem and Guijiang rivers. SO_4^{2-} is the second dominant anion with a concentration between 0.047 and 0.310 mmol/L. Cl^- ranges from 0.031–0.256 mmol/L and the highest values occur in the Luoding. NO_3^- concentration varies basically between 0.011 and 0.132 mmol/L except for a value of 0.408 mmol/L (Xj-1). On average, the sum of the three anions (SO_4^{2-}, Cl^- and NO_3^-) accounts for 16% of the total anions, where SO_4^{2-} alone accounts for 7%.
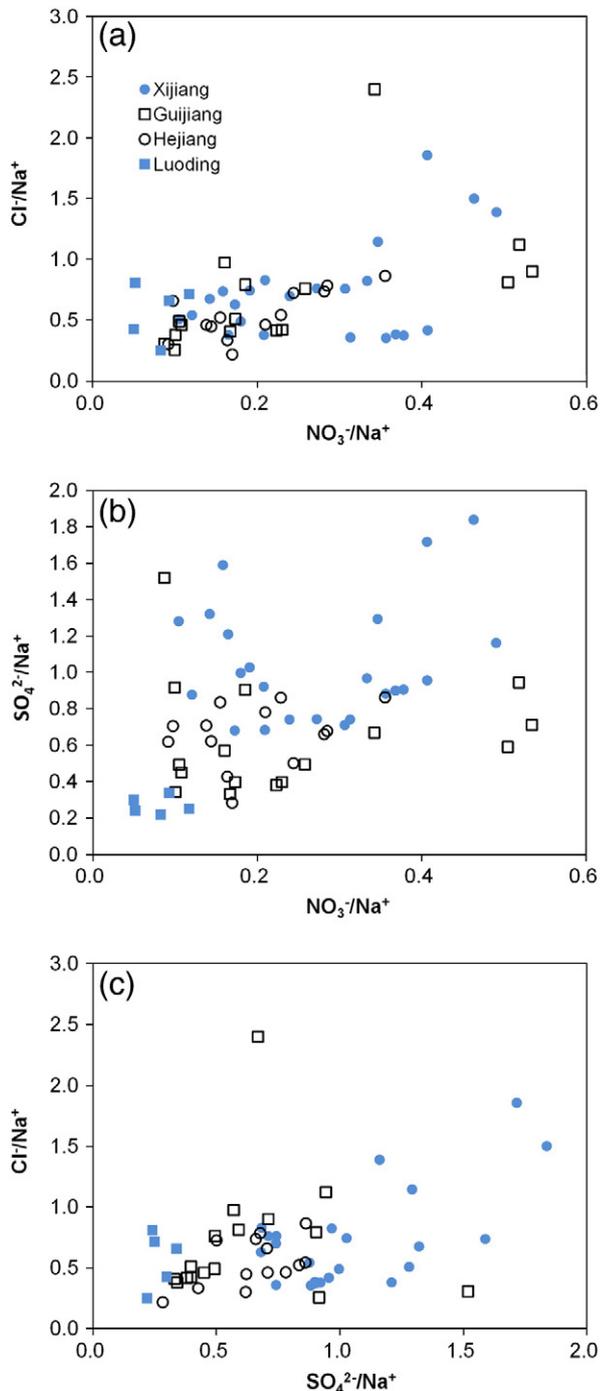
Fig. 6. Ion ratios of the river waters in the four subcatchments. (a) NO_3^-/Na^+ versus SO_4^{2-}/Na^+, and (b) Cl^-/Na^+ versus SO_4^{2-}/Na^+.

Dissolved Silica is mainly derived from silicate weathering, which may partly be consumed by diatoms (Turner and Rabalais, 1991). The mean concentrations of dissolved silica is 0.121 mmol/L in the Xijiang stem, 0.122 mmol/L in the Guijiang, 0.120 mmlol/L in the Hejiang and 0.206 mmol/L in the Luoding.

4.2. Spatial and seasonal variations in major ion concentrations

It is notable that both the pH value and $Ca^{2+} + Mg^{2+}$ concentrations consistently follow an order of Guijiang ≥ Xijiang > Hejiang > Luoding, whereas K^+ and Na^+ show a reversed order, i.e. Guijiang ≤ Xijiang < Hejiang < Luoding. Based on the rock type distribution map of the Zhujiang catchment, carbonate accounts for 42.5%, 50.8%, and 23.2% in the Xijiang, Guijiang, and Hejiang subcatchments, respectively, and little carbonate in the Luoding. This suggests a dominant impact of the bedrock weathering on the water chemistry. Both SO_4^{2-} and Cl^- concentrations are fairly higher in the Xijiang stem than in its three tributaries, indicating a prominent anthropogenic influence in the upper reaches of the Xiijang.

The concentrations of Ca^{2+}, Mg^{2+}, and HCO_3^- in the Guijiang and Hejiang all show a decline trend from the upper to the lower, while Si concentrations show a reverse trend (Fig. 3). This pattern accords well to the distribution of carbonate that is exposed only in the upper reaches (Fig. 1). SO_4^{2-} concentrations in the Hejiang also decrease from upper to the lower river, consistent with the fact that intensive activities of both agriculture and industry and cities with large population all are located in the upper area of the sampling sites. SO_4^{2-} in the Guijiang shows a similar downstream decreasing pattern, very likely attributable to the paper factories and chemical plants in the upper reaches.

The four study tributaries of the Xijiang river display a similar seasonal variation pattern in major ion concentrations. The highest major ion concentration and TDS occur in December (winter), while the lowest in June (summer). In December, as the regional precipitation is at the lowest level of a year, the river discharge possibly comes mainly from subsurface flow, which could result in a longer time of water/rock interaction and thus greater dissolution of the solids. Samples in June were taken from the waning period of an extremely big flood event (Fig. 2), and thus have lower values of major ion concentrations due to the flood scavenging. In mid July, the discharge level is high, and the solute concentration is also fairly high, possibly due to higher temperature that could promote rapid dissolution of minerals and result in a higher soil CO_2 concentration thus enhancing the solubility of the rocks.

It is interesting that the dissolved Si concentration in the Xijiang stem, Guijiang and Hejiang show a reverse trend (higher in wet season than in dry season) compared with other main components such as Ca^{2+}, Mg^{2+} and HCO_3^-. This is also reported by a previous study (Gao et al, 2009). As is explained in that study, the dissolved Si is mainly preserved in the surface siliceous soil in carbonate region and flushed out by surface water that dominates the river water during flooding season. For the Luoding, a silicate-dominated river, dissolved silicate is diluted rather than concentrated in the wet season.

5. Discussions

5.1. Sources of major ions

Possible sources of major ion species in the surface water are weathering of rocks, atmospheric precipitation, evaporation–crystallization, and anthropogenic inputs (Gibbs, 1970). Major ion composition displayed by the ternary plots (Fig. 4) suggests that carbonate rock weathering dominates the water chemistry of the Xijiang river.

The relative importance of various possible sources for the major ions is stoichiometrically examined below. In Fig. 5a, the data points deviate from and scatter above the 1:1 trend line, suggesting that chloride evaporite weathering is not a significant source. This is
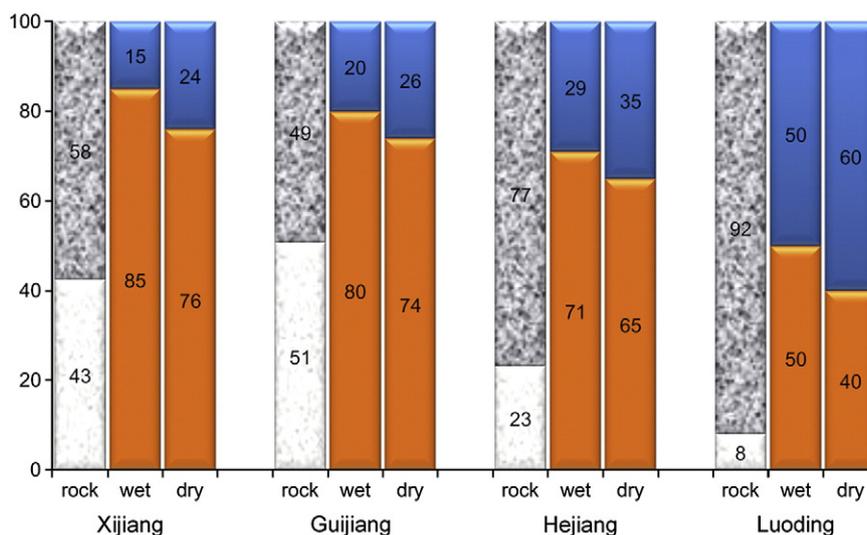
Fig. 7. Estimated percentage contributions (the right-side column in each subcatchment) of silicate (the upper bar) and carbonate (the lower bar) weathering to bicarbonate flux of the rivers. The left-side bar shows the percentages of silicate (the upper bar) and carbonate (the lower bar) in the bedrock.

consistent with the fact that no evaporate has been found in the river basin. Therefore, the Cl^- should mainly derive from atmospheric input or residential and industrial wastes. The excess K^+ and Na^+ to Cl^- should derive from sodium and potassium aluminosilicates weathering. Fig. 5b shows that sulfate weathering is less relevant to the Ca^{2+} and Mg^{2+}. In Fig. 5c, all the samples approach to the 1:1 line, demonstrating the dominant impact of carbonate and/or silicate weathering in the Xijiang river. It is possible that the slightly excess Ca^{2+} and/or Mg^{2+} (above the 1:1 line in Fig. 5c) may be attributed to sulfates, or HCO_3^- decomposition by input of other acidic matter. When SO_4^{2-} is incorporated, the samples are further closer to the 1:1 line (Fig. 5d), suggesting some influence of sulfate. Sulfate may come mainly from three sources: (1) dissolution of gypsum; (2) oxidation of pyrite in rocks and (3) anthropogenic input, such as acid rains and fertilizers. In the upper Xijiang, river water is rich in sulfate ions, ranging from 0.134 to 2.146 mmol/L (mean: 0.660 mmol/L) (Li et al., 2008). The coal-combustion industry and mining of high-sulfide coal in the Beipanjiang and Nanpanjiang catchments with severe acid rains in the upper reaches could be responsible for abundance of riverine sulfate (Han and Liu, 2004; Li et al., 2008). In the lower Xijiang, sulfate ion has been greatly diluted, ranging from 0.047 to 0.310 mmol/L (mean: 0.133 mmol/L).

Sulfate, nitrate and chloride ions in river water can be mainly or partly derived from communal inputs including residential and industrial wastes, agricultural fertilizers and atmospheric input by pollution. Particularly NO_3^- is most likely of anthropogenic origin. In this study, positive relationships are detected between molar ratios of NO_3^-/Na^+ and SO_4^{2-}/Na^+, Cl^-/Na^+ and SO_4^{2-}/Na^+, and Cl^-/Na^+ and NO_3^-/Na^+ (see Fig. 6), suggesting some anthropogenic origin of the Cl^- and SO_4^{2-}. Because the three anions only account for a minor part of the TDS, the anthropogenic and atmospheric influences (including rainwater input) should be rather small.

5.2. Contributions of carbonate and silicate sources to the major ions

Chemical weathering of carbonate and silicate rocks with carbonic acid has been investigated by numerous studies (e.g. Berner et al., 1983; Gaillardet et al., 1999; Mortatti and Probst, 2003; Chetelat et al., 2008). CO_2 is a natural acid and is the most significant reactant in rock weathering. Recently, the importance of sulfuric acid in chemical weathering has been addressed (Galy and France-Lanord, 1999; Calmels et al., 2007; Lerman et al., 2007; Xu and Liu, 2007; Li et al., 2008; Han et al., 2010). Reactions of H_2SO_4 with carbonate minerals may produce

bicarbonate without CO_2 consumption, or even release CO_2 in different stoichiometric proportions.

$$2CaCO_3 + H_2SO_4 = 2Ca^{2+} + 2HCO_3^- + SO_4^{2-} \qquad (1)$$

$$CaCO_3 + H_2SO_4 = Ca^{2+} + SO_4^2 - + H_2O + CO_2 \qquad (2)$$
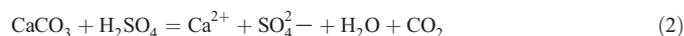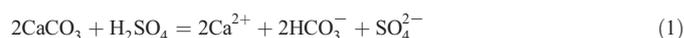
Reaction (1) occurs in the case of neutralization of sulfuric acid. When a solution is in low pH level and is dominated by sulfuric acid mixing with carbonate-saturated water, for example, acid rain occurs in carbonate region, reaction (2) takes place. But this is not the typical case in the Xijiang basin (Xu and Liu, 2007; Li et al., 2008).

Collectively, these processes can be largely described by the following stoichiometric equations in mmol/L.

$$HCO_3\_carb = 2Ca\_carb - carb + 2Mg\_carb + Ca\_carb - sulf \qquad (3)$$

$$HCO_3\_sil = Na\_sil + K\_sil + 2Ca\_sil + 2Mg\_sil \qquad (4)$$

The subscripts carb and sil denote for carbonate and silicate origin, respectively. HCO$_3$_carb represents the bicarbonate from carbonate weathering and HCO$_3$_sil from silicate weathering. Ca_carb-carb and Ca_carb-sulf denote the calcium sourced from reactions of carbonate respectively with carbonic acids and sulfuric acids.

Based on Eqs. (3) and (4), it is possible to estimate the contributions of carbonate and silicate sources to the major ions in the river water. For a first order estimation, we assume that:

- all the chloride anion is from atmospheric salt and anthropogenic inputs;
- all the sodium is derived from silicate rock weathering (Na_sil) after subtraction of chloride origin;
- all potassium is derived from silicate weathering (K_sil);
- calcium and magnesium are derived from carbonate (Ca_carb and Mg_carb) and silicate weathering (Ca_sil and Mg_sil); and
- all SO_4^{2-} is derived from sulfide oxidation and anthropogenic inputs.

According to the lowest chloride concentration of the samples, the chloride from atmospheric input is estimated to be 0.031 mmol/L (GJ-2, collected on July 1). Then the Na^+ and K^+ released by silicate weathering become known. The amounts of Ca^{2+} and Mg^{2+} from carbonate and silicate dissolution can be evaluated by the ionic ratios

Ca/Na = 0.4 and Mg/Na = 0.2, which were obtained by Zhang et al. (2007) from rivers draining virtually a pure silicate terrain in this region. As silicate weathering in the study area is not significant in comparison with carbonate weathering, it is assumed that all SO_4^{2-} is involved in the carbonate–H_2SO_4 reaction and balanced by Ca^{2+} in the river water. According to Eq. (1), the amount of Ca^{2+} from carbonate dissolution by sulfuric acid is equivalent to 2-fold of SO_4^{2-}. After subtraction of Ca^{2+} produced by silicate weathering (Ca_sil) and carbonate weathering with sulfuric acids (Ca_carb-sulf) from the measured Ca^{2+} for the river water, the remaining is the fraction of Ca^{2+} from carbonate weathering by carbonic acid (Ca_carb-carb). Based on above equations, the contributions of carbonate and silicate weathering to the HCO_3^- are calculated for each river using the data measured at the river outlets (XJ-1 for the Xijiang, GJ-1 for the Guijiang, HJ-1 for the Hejiang and LD for the Luoding). For seasonal comparison, data obtained in April and December are averaged for dry season, and data of May, June and July are averaged for wet season.

The computed results (Fig. 7) indicate that carbonate weathering contributes 70–81% to the riverine bicarbonate in the Xijiang except for the Luoding with a mean value of 45%, and show an order of

Table 2
Chemical compositions of river water in the Xijiang basin.

Sample	Date	pH	Tem	Flow	K⁺	Ca²⁺	Na⁺	Mg²⁺	Si	SO₄²⁻	NO₃⁻	Cl⁻	HCO₃⁻	TDS	SIc[a]
	dd-mm		(°C)	(m³/s)	(mmol/L)									(mg/L)	
XJ-1	17-Apr	7.57	21.9	2020	0.036	0.610	0.142	0.220	0.097	0.137	0.047	0.117	1.566	156	−0.479
XJ-2	17-Apr	7.83	21.7	2020	0.034	0.613	0.159	0.201	0.106	0.118	0.043	0.121	1.515	151	−0.252
XJ-3	17-Apr	7.79	21.6	2020	0.033	0.578	0.159	0.188	0.111	0.109	0.033	0.132	1.414	143	−0.343
XJ-4	17-Apr	7.86	21.5	2020	0.031	0.633	0.145	0.192	0.100	0.103	0.044	0.110	1.586	154	−0.189
XJ-5	17-Apr	7.82	21.8	2020	0.034	0.688	0.181	0.236	0.104	0.134	0.043	0.127	1.667	167	−0.174
GJ-1	14-Apr	7.41	17.8	80	0.022	0.580	0.088	0.140	0.096	0.052	0.044	0.072	1.465	135	−0.749
GJ-2	14-Apr	7.53	18.6	80	0.021	0.602	0.081	0.145	0.089	0.058	0.043	0.073	1.515	139	−0.575
GJ-3	14-Apr	7.89	18.5	80	0.022	0.606	0.101	0.149	0.085	0.050	0.026	0.077	1.535	139	−0.133
GJ-4	14-Apr	8.04	18.7	80	0.021	0.687	0.089	0.152	0.083	0.059	0.030	0.213	1.667	156	0.075
HJ-1	16-Apr	7.02	21.5	117	0.035	0.361	0.132	0.131	0.131	0.066	0.032	0.096	0.859	94	−1.503
HJ-2	16-Apr	7.07	20.8	117	0.031	0.486	0.133	0.157	0.133	0.090	0.038	0.104	1.141	120	−1.226
HJ-3	16-Apr	7.13	20.6	117	0.030	0.497	0.138	0.157	0.138	0.091	0.039	0.102	1.162	122	−1.152
LD	18-Apr	7.64	22	26	0.056	0.535	0.285	0.184	0.193	0.071	0.033	0.204	1.566	158	−0.429
XJ-1	15-May	7.89	23.4	4890	0.049	0.850	0.144	0.216	0.118	0.186	0.050	0.165	1.860	192	0.046
XJ-2	15-May	7.79	23.5	4890	0.051	0.873	0.108	0.222	0.116	0.198	0.050	0.162	1.736	185	−0.070
XJ-3	15-May	7.85	24	4890	0.036	0.856	0.102	0.172	0.111	0.118	0.050	0.141	1.947	187	0.043
XJ-4	15-May	7.86	23.5	4890	0.059	1.007	0.138	0.264	0.122	0.237	0.056	0.256	2.046	220	0.119
GJ-1	15-May	7.53	23.4	656	0.032	0.846	0.087	0.139	0.106	0.082	0.045	0.097	1.798	171	−0.312
HJ-1	15-May	6.99	23.8	423	0.032	0.501	0.084	0.091	0.139	0.073	0.030	0.073	1.054	109	−1.276
LD	18-May	7.36	24	40	0.086	0.458	0.323	0.112	0.194	0.109	0.030	0.213	1.153	134	−0.913
XJ-1	2-Jul	7.35	25	26,050	0.036	0.615	0.102	0.134	0.136	0.105	0.019	0.076	1.350	136	−0.717
XJ-2	2-Jul	7.33	25.1	26,050	0.037	0.631	0.107	0.140	0.136	0.073	0.019	0.067	1.420	138	−0.703
XJ-3	2-Jul	7.22	25	26,050	0.035	0.607	0.098	0.134	0.130	0.156	0.016	0.072	1.350	140	−0.856
XJ-4	2-Jul	7.21	25	26,050	0.039	0.637	0.144	0.140	0.133	0.132	0.030	0.054	1.390	143	−0.832
XJ-5	2-Jul	7.22	25.1	26,050	0.035	0.668	0.169	0.145	0.135	0.205	0.028	0.064	1.500	159	−0.778
GJ-1	1-Jul	7.14	24.4	809	0.034	0.394	0.108	0.092	0.177	0.048	0.012	0.049	0.930	96	−1.266
GJ-2	1-Jul	7.14	24.4	809	0.033	0.389	0.124	0.084	0.167	0.113	0.012	0.031	0.900	99	−1.291
GJ-3	1-Jul	7.16	24.4	809	0.032	0.394	0.125	0.084	0.154	0.189	0.011	0.038	0.930	108	−1.260
HJ-1	30-Jun	6.94	24.9	97	0.035	0.282	0.185	0.084	0.119	0.052	0.031	0.040	0.680	76	−1.729
HJ-2	30-Jun	7.37	25.1	97	0.037	0.441	0.170	0.113	0.121	0.073	0.028	0.057	0.980	104	−0.963
HJ-3	30-Jun	7.32	24.5	97	0.037	0.434	0.153	0.114	0.117	0.095	0.014	0.046	0.980	103	−1.030
LD	27-Jun	7.38	25	76	0.084	0.315	0.228	0.092	0.192	0.055	0.012	0.184	0.930	104	−1.115
XJ-1	13-Jul	7.09	26	7920	0.046	0.732	0.129	0.285	0.144	0.165	0.014	0.065	1.872	183	−0.767
XJ-2	13-Jul	7.28	26	7920	0.046	0.775	0.132	0.299	0.133	0.116	0.016	0.071	1.922	183	−0.541
XJ-3	13-Jul	7.39	25.8	7920	0.041	0.749	0.129	0.286	0.132	0.128	0.023	0.063	1.996	187	−0.435
XJ-4	13-Jul	7.65	25.7	7920	0.041	0.793	0.110	0.307	0.132	0.146	0.016	0.074	2.058	194	−0.144
XJ-5	13-Jul	7.98	26.7	7920	0.041	0.865	0.119	0.339	0.132	0.167	0.408	0.108	2.306	241	0.272
GJ-1	15-Jul	7.57	25.8	415	0.037	0.437	0.115	0.196	0.174	0.056	0.012	0.056	1.240	120	−0.662
GJ-2	15-Jul	7.96	26	415	0.039	0.452	0.118	0.197	0.153	0.047	0.020	0.060	1.277	122	−0.247
GJ-3	15-Jul	7.96	25.5	415	0.039	0.509	0.107	0.213	0.154	0.097	0.020	0.085	1.438	140	−0.162
GJ-4	15-Jul	7.96	25.2	415	0.045	0.521	0.121	0.220	0.139	0.069	0.019	0.118	1.451	140	−0.152
HJ-1	14-Jul	7.95	25.8	204	0.045	0.331	0.126	0.177	0.136	0.089	0.012	0.083	0.967	102	−0.508
HJ-2	14-Jul	7.72	25.3	204	0.044	0.459	0.132	0.220	0.108	0.110	0.020	0.069	1.240	125	−0.507
HJ-3	14-Jul	7.89	25.5	204	0.045	0.487	0.131	0.229	0.106	0.113	0.030	0.071	1.277	129	−0.300
LD	19-Jul	6.93	24.3	20	0.087	0.393	0.277	0.184	0.210	0.083	0.014	0.118	1.240	131	−1.370
XJ-1	13-Dec	7.68	20.2	1610	0.069	0.992	0.339	0.303	0.122	0.299	0.121	0.119	2.071	232	−0.113
XJ-2	13-Dec	7.8	19.8	1610	0.073	1.012	0.326	0.311	0.114	0.293	0.120	0.125	2.180	238	0.029
XJ-3	13-Dec	7.74	19.5	1610	0.073	1.008	0.334	0.311	0.113	0.303	0.126	0.125	2.235	243	−0.025
XJ-4	13-Dec	7.83	19.6	1610	0.073	0.942	0.367	0.293	0.110	0.272	0.115	0.131	2.104	229	0.014
XJ-5	13-Dec	7.84	19	1610	0.071	1.068	0.325	0.326	0.107	0.310	0.132	0.135	2.256	248	0.091
GJ-1	16-Dec	7.92	19.2	18	0.051	0.615	0.343	0.183	0.096	0.117	0.035	0.130	1.526	156	−0.194
GJ-2	16-Dec	8.03	19.2	18	0.067	0.722	0.413	0.196	0.097	0.136	0.069	0.168	1.744	181	0.031
GJ-3	16-Dec	8.19	19.2	18	0.071	0.735	0.358	0.186	0.097	0.136	0.080	0.148	1.744	180	0.195
GJ-4	16-Dec	8.04	19.6	18	0.069	0.762	0.351	0.190	0.088	0.140	0.081	0.148	1.766	183	0.074
HJ-1	14-Dec	7.97	19.2	167	0.067	0.525	0.319	0.170	0.129	0.198	0.046	0.143	1.145	140	−0.335
HJ-2	14-Dec	8.06	18.6	167	0.071	0.780	0.374	0.234	0.099	0.265	0.052	0.172	1.581	185	0.032
HJ-3	14-Dec	8.02	18.7	167	0.068	0.781	0.383	0.215	0.089	0.299	0.080	0.177	1.363	176	−0.070
LD	19-Dec	7.41	14.8	40	0.082	0.253	0.451	0.108	0.238	0.098	0.037	0.112	0.948	114	−1.328

[a] SIc is the calcite saturation index calculated using PHREEQC.

Table 3
Chemical weathering rates and CO_2 consumption rates in the lower Xijiang basin.

Subasin	TDS_carb		TDS_sil		TDS_total		CO_2_sil		CO_2_carb		CO_2_total	
	10^6 t/yr	t/km²/yr	10^6 t/yr	t/km²/yr	10^6 t/yr	t/km²/yr	10^9 mol/yr	10^5 mol/km²/yr	10^9 mol/yr	10^5 mol/km²/yr	10^9 mol/yr	10^5 mol/km²/yr
Xijiang	19.6	130.9	3.3	16.6	22.9	65.2	78.1	3.9	126.2	8.4	204.3	5.8
Guijiang	1.1	117.1	0.3	29.0	1.3	73.7	6.0	6.7	8.1	8.6	14.0	7.7
Hejiang	0.4	148.6	0.1	11.2	0.6	52.6	3.2	3.6	2.5	9.1	5.7	4.9
Luoding	0.1	394.9	0.1	25.3	0.2	62.6	1.8	6.2	0.5	20.5	2.4	7.5

Note: The subscripts carb, sil and total denote the contributions made by carbonate, silicate and the total of silicate and carbonate, respectively. Values for the Xijiang represent the entire Xijiang basin, including the Guijiang, Hejiang and Luoding.

Xijiang>Guijiang>Hejiang>Luoding, generally in agreement with the order of the ratios of carbonate/silicate area in these subbasins. It is noted that Guijiang has a higher carbonate proportion but a lower carbonate-sourced HCO_3^- than the Xijiang. This discrepancy could be explained by the difference in topography (see slope in Table 1). For terrains with a same area on plan maps, steeper slopes imply more exposing surface and thus more rainwater–rock interaction than flatter slopes.

A greater percentage contribution of carbonate dissolution to HCO_3^- has been observed in wet season (summer) than dry season (winter) in the four tributaries, indicating a possible effect of increasing temperature on acceleration of chemical weathering, as has been discussed in Section 4.2. The calculated saturation index of carbonate (SIc) (see Table 2) indicates that HCO_3^- in winter is closer to saturation than in summer, thus has less potential for the increase of

concentration than in summer, leading to a higher percentage contribution in wet season (summer) than in dry season (winter). This could also explain a relatively higher percentage contribution of silicate weathering in winter than in summer (see Fig. 7).

5.3. Chemical weathering rates and associated CO_2 consumption

The quantities of chemical weathering for carbonate (TDS_carb) and silicate (TDS_sil) can be calculated from water chemical data (in mg/L) by the following equations:

$$TDS\_carb-carb = Ca\_carb-carb + Mg\_carb + 0.5HCO_3\_carb-carb \quad (5)$$

$$TDS\_carb-sulf = Ca\_carb-sulf + HCO_3\_carb-sulf \quad (6)$$
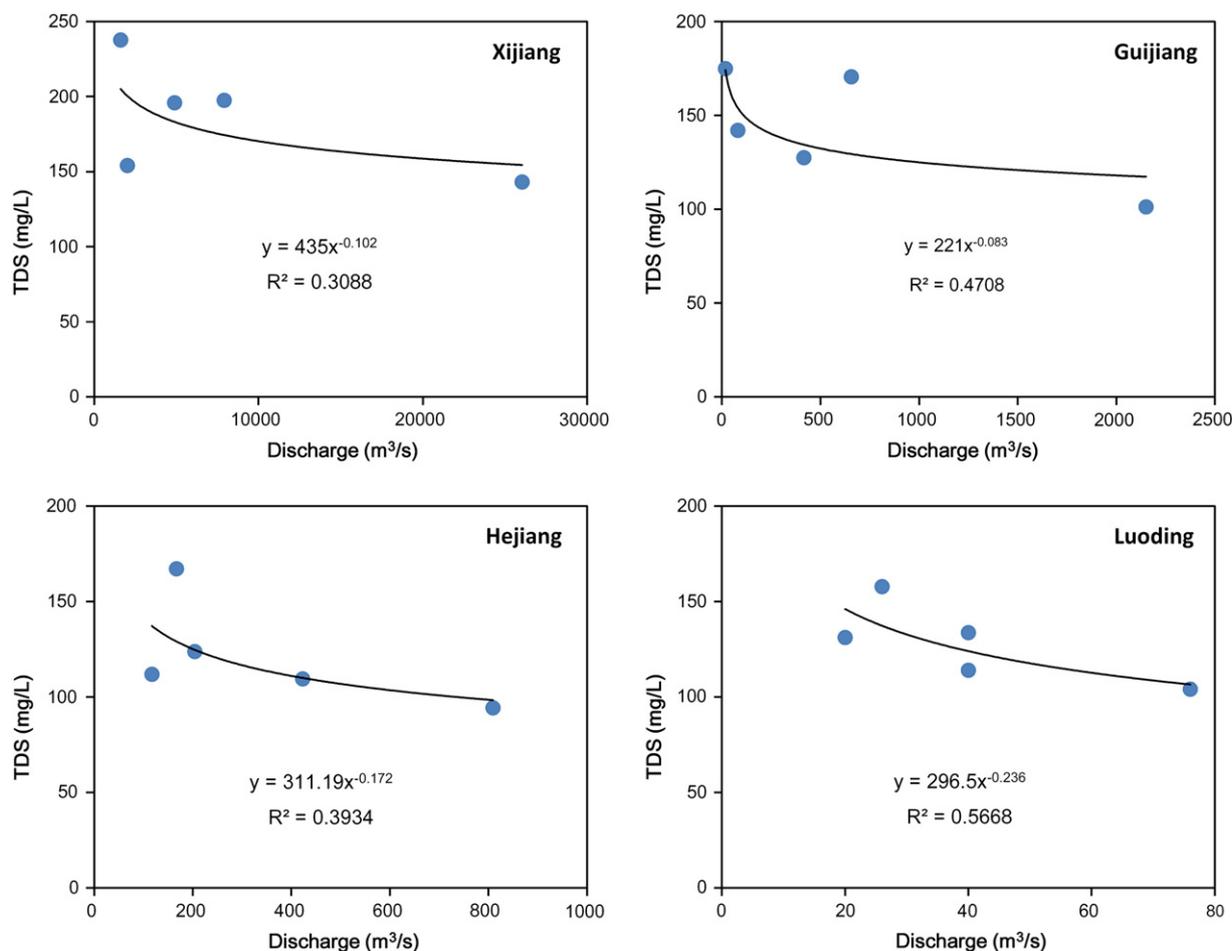
Fig. 8. Relationship between total dissolved solids (TDS) and discharge. Seasonal concentrations of TDS for each river are averaged on spatial samples.
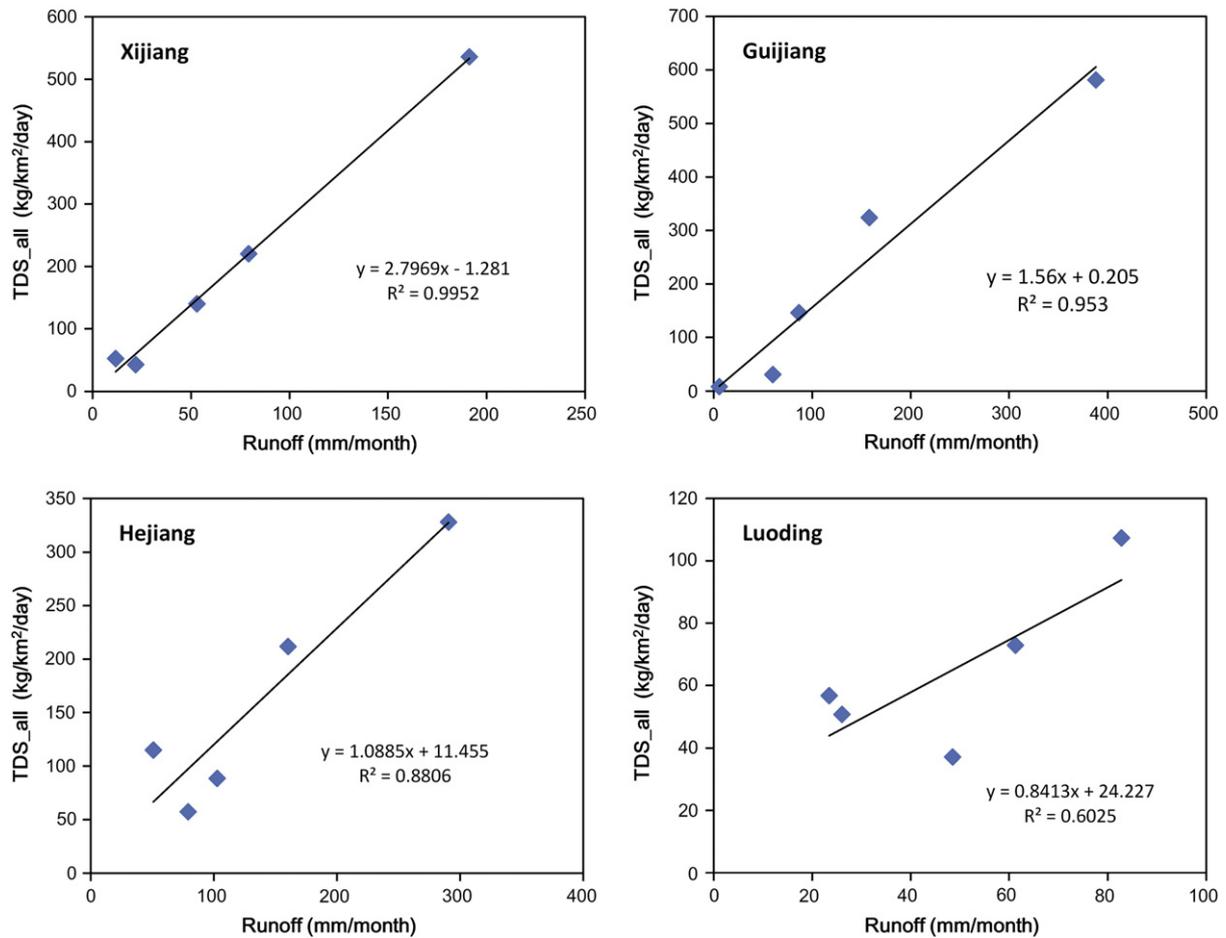
Fig. 9. Relationship between chemical weathering rate and runoff. Seasonal chemical weathering rate is calculated by mean sample value multiplying daily discharge on the sampling date. Seasonal runoff is calculated from the daily discharge divided by drainage basin area.

$$TDS\_carb = TDS\_carb{-}carb + TDS\_carb{-}sulf \tag{7}$$

$$TDS\_sil = Ca\_sil + Mg\_sil + K\_sil + Na\_sil + SiO_2\_sil \tag{8}$$

Where TDS_carb-carb, TDS_carb-sulf represent the chemical weathering budget for carbonate with carbonic and sulfuric acid, respectively. HCO$_3$_carb-carb and HCO$_3$_carb-sulf are bicarbonate ion from carbonate weathering respectively by carbonic and sulfuric acids, and can be obtained from Eq. (3). SiO$_2$_sil is the aqueous silica derived from silicate weathering.

During silicate weathering, all HCO$_3^-$ produced is from atmospheric/soil CO$_2$. For carbonate dissolution by carbonic acid, only half amount of HCO$_3^-$ is from atmospheric/soil CO$_2$, but no HCO$_3^-$ is produced from atmospheric/soil CO$_2$ during carbonate dissolution by sulfuric acid. Therefore, the total CO$_2$ (R$_{CO2}$) consumed by rock weathering can be calculated by the following equation:

$$R_{CO2} = HCO_3\_sil + 0.5HCO_3\_carb{-}carb \tag{9}$$

Based on above equations, the chemical weathering rates and CO$_2$ consumption fluxes by carbonate and silicate weathering can be estimated with water discharge and water geochemical data measured at river outlets (Table 3). The data from sampling site XJ-1 represent the entire Xijiang basin, including contributions from the Guijiang, Hejiang and Luoding. Due to small discharges of the three tributaries, thus small influence to the water geochemistry of the Xijiang stem, it could be still meaningful to compare the Xijiang at XJ-1 (where a complete daily to yearly hydrometric dataset is available) with the three tributaries.

Carbonate weathering rate was calculated to be 130.9 t/km^2/yr (divided by carbonate area) for Xijiang, 117.1 t/km^2/yr for Guijiang, 148.6 t/km^2/yr for Hejiang, and 394.9 t/km^2/yr for the Luoding basins. Carbonate weathering by sulfuric acid contributes 23–32% to the total rock weathering in the river basin, which suggests a significant influence of sulfuric acid in rock chemical weathering in the study region.

Silicate weathering rate is about 16.6 t/km^2/yr (divided by silicate rock area) in the Xijiang, 29.0 t/km^2/yr in Guijiang, 11.2 t/km^2/yr in Hejiang, and 25.3 t/km^2/yr in Luoding basins. These rates are comparable to those for Amazon (23 t/km^2/yr, Mortatti and Probst, 2003), but higher than those for Nile (0.8 t/km^2/yr) and Congo (4.3 t/km^2/yr) basins (Gaillardet et al., 1999).

The weathering rates of carbonate are 5–20 times (in t/km^2/yr) higher than silicates in the Xijiang basin. On average, the total chemical (carbonate and silicates) weathering rate is about 65.2 t/km^2/yr in Xijiang, 73.7 t/km^2/yr in Guijiang, 52.6 t/km^2/yr in Hejiang, and 62.6 t/km^2/yr in Luoding basins.

In the Xijiang basin, the total annual consumption of CO$_2$ by rock weathering is 2.0×10^{11} mol/yr (5.8×10^5 mol/km^2/yr) with more than 60% by carbonate weathering. As very little carbonate in the Luoding catchment, carbonate weathering contributes a much smaller portion (22%) to the total CO$_2$ consumption for this catchment.

The area specific CO$_2$ consumption rates by carbonate weathering in the Xijiang basin range from 8.4 to 20.5×10^5 mol/km^2/yr (divided

by carbonate area), higher than the estimate of 8×10^5 mol/km^2/yr for global-scaled carbonate weathering (Meybeck, 1987). The CO_2 consumption through silicate weathering is 3.6–6.7×10^5 mol/km^2/yr (divided by silicate rock area) in the Xijiang basin, higher than that in many world rivers such as the Amazon (1.7×10^5 mol/km^2/yr, Mortatti and Probst, 2003) and the Niger (0.3–1×10^5 mol/km^2/yr, Picouet et al, 2002). According to previous study (Gao et al., 2009), the CO_2 flux consumed by carbonate and silicate weathering within the Xijiang basin surveyed at Wuzhou (Fig. 1) are 1.7×10^{11} mol/yr and 0.6×10^{11} mol/yr, respectively, very close to the results obtained by this study (see Table 3).

Carbonate weathering with sulfuric acid may lead to a net source to the atmospheric CO_2, because precipitation of calcite in the ocean releases CO_2 that has not been consumed on land. Based on the mean sulfate concentration in the river water, the fluxes of CO_2 released to the atmosphere–ocean system by sulfuric acid-induced carbonate weathering are 3.7×10^{10} mol/yr or 1.1×10^5 mol/km^2/yr for Xijiang, 1.4×10^9 mol/yr or 0.77×10^5 mol/km^2/yr for Guijiang, 1.0×10^9 mol/yr or 0.86×10^5 mol/km^2/yr for Hejiang and 0.21×10^9 mol/yr or 0.68×10^5 mol/km^2/yr for Luoding. These fluxes are relatively lower than that for the upper Xijiang region (1.6×10^5 mol/km^2/yr, Li et al., 2008), and are comparable with the CO_2 flux consumed by silicate weathering.

5.4. Relationship between chemical weathering rates and environmental factors

The major ion concentrations in the river water generally decrease exponentially with increasing discharge or runoff. In the Xijiang basin, the power of the regression fits for the TDS-discharge ranges from -0.24 to -0.08 (Fig. 8), consistent with the value of -0.4 to 0 for majority of world rivers (Walling and Webb, 1986). Compared with the change in discharge, TDS concentration varied with smaller amplitudes. This is also true during the extreme flood event occurred in the Xijiang in May 2005 (Sun et al., 2007; Gao et al., 2009), indicating that large amount of solute is provided by increased river discharge, and increasing discharge/runoff must increase chemical weathering. Among different basins, chemical weathering rates are also positively related to runoff (Fig. 9). However, the relationship between runoff and chemical weathering rates seems nonlinear; other factors such as temperature and duration of water–rock contact should be taken into account. For the Xijiang basin, the highest values of major ion concentrations are observed in December and July. For the higher concentration in July, higher temperature is possibly the major factor. As discussed in Section 4.2, higher temperatures will result in rapid dissolution and a higher soil CO_2 concentration thus an increase of mineral solubility. In December, river water with the lowest temperature in a year reaches the solute saturation state (SIc) (Table 2). In the Luoding, it is found that solute concentrations in May are evidently higher than those in December with the same amount of water discharge, which should be attributed to a lower biogenic activity thus lower soil CO_2 level caused by lower temperature in winter.

In the Nanpanjiang and Beipanjiang basins, the upper regions of the Xijiang (Fig. 1), the total consumption flux of atmospheric CO_2 by carbonate and silicate weathering are calculated as 6.9–8.7×10^5 mol/km^2/yr, and more than 85% by carbonate weathering (Xu and Liu, 2007). Compared with the lower Xijiang, more contribution of carbonate weathering to the CO_2 consumption flux in the upper region can be explained by the higher percentage (about 60%) of carbonate area in the Nanpanjiang and Beipanjiang basins. If compared with the lower Xijiang, however, the weathering rate in these basins is under-proportionally increased with the carbonate area, for which, less precipitation (800–1200 mm/yr) and lower air temperature (10–15 °C) might be responsible.

6. Conclusions

Water geochemistry of the Xijiang stem river and its 3 tributaries is dominated by Ca^{2+} and HCO_3^-, accounting for more than 60% of total cations and 80% of total anions. Spatial variations of major ion concentrations among the subbasins and along the river courses are consistent with the distribution of bedrock type, i.e. the ratio of carbonate versus silicate. Major ion concentrations are lower during rainy season and higher during dry season. Stoichiometric analysis and molar ratios of SO_4^{2-}/Na^+, Cl^-/Na^+ and NO_3^-/Na^+ indicate some, but minor, anthropogenic influence on the water chemistry of the Xijiang river.

Chemical weathering rates range from 52.6 t/km^2/yr to 73.7 t/km^2/yr within the lower Xijiang. Carbonate weathering rate is over one order higher in magnitude than silicates. CO_2 consumption rate by rock weathering is 2.0×10^{11} mol/yr, of which more than 60% is contributed by carbonate weathering. The flux of CO_2 released to the atmosphere–ocean system by sulfuric acid-induced carbonate weathering is 3.7×10^{10} mol/yr (1.1×10^5 mol/km^2/yr) for the Xijiang, which is comparable with the CO_2 flux consumed by silicate weathering. The results show that the Xijiang basin is one of the most intensive chemical weathering regions around the world. Runoff/rainfall is the first controlling factor for the weathering rate in the basin. Increases in temperature and water–rock contact duration may significantly enhance chemical weathering rate.

References

Amiotte-Suchet P, Probst JL, Ludwig W. Worldwide distribution of continental rock lithology: implications for the atmospheric/soil CO_2 uptake by continental weathering and alkalinity river transport to the oceans. Glob Biogeochem Cycles 2003;17:1891–903.

Berner RA, Lasaga AC, Garrels RM. The carbonate-silicate geochemical cycle and its effect on atmospheric carbondioxide over the past 100 million years. Am J Sci 1983;284:641–83.

Caldeira K. Long term control of atmospheric carbon dioxide: low temperature seafloor alteration or terrestrial silicate-rock weathering? Am J Sci 1995;295:1077–114.

Calmels D, Gaillardet J, Brenot A, France-Lanord C. Sustained sulfide oxidation by physical erosion processes in the Mackenzie River basin: climatic perspectives. Geology 2007;35:1003–6.

Chen J, He D. Chemical characteristics and genesis of major ions in the Pearl River Basin. Acta Sci Nat Univ Pekinensi 1999;35:786–93 (in Chinese).

Chetelat B, Liu CQ, Zhao ZQ, Wang QL, Li SL, Li J, et al. Geochemistry of the dissolved load of the Changjiang Basin rivers: anthropogenic impacts and chemical weathering. Geochim Cosmochim Acta 2008;72:4254–77.

Dalai TK, Krishnaswami S, Sarin MM. Major ion chemistry in the headwaters of the Yamuna river system: chemical weathering, its temperature dependence and CO_2 consumption in the Himalaya. Geochim Cosmochim Acta 2002;66:3397–416.

Dessert C, Dupré B, Francois LM, Schott J, Gaillardet J, Charkrapani G, et al. Erosion of Deccan Traps determined by river geochemistry: impact on the global climate and the $^{87}Sr/^{86}Sr$ ration of seawater. Earth Planet Sci Lett 2001;188:459–74.

Gaillardet J, Dupré B, Louvat P, Allégre CJ. Global silicate weathering and CO_2 consumption rates deduced from the chemistry of large rivers. Chem Geol 1999;159:3-30.

Galy A, France-Lanord C. Weathering processes in the Ganges–Brahmaputra basin and the riverine alkalinity budget. Chem Geol 1999;159:31–69.

Gao Q, Tao Z, Huang X, Nan L, Yu K, Wang Z. Chemical weathering and CO_2 consumption in the Xijiang River basin, South China. Geomorphology 2009;106:324–32.

Gibbs RJ. Mechanisms controlling world water chemistry. Science 1970;170:1088–90.

Grasby SE, Hutcheon I. Chemical dynamics and weathering rates of a carbonate basin Bow River, Southern Alberta. Appl Geochem 2000;15:67–77.

Hagedorn B, Cartwright I. Climatic and lithologic controls on the temporal and spatial variability of CO_2 consumption via chemical weathering: an example from the Australian Victorian Alps. Chem Geol 2009;260:234–53.

Han G, Tang Y, Xu Z. Fluvial geochemistry of rivers draining karst terrain in Southwest China. J Asian Earth Sci 2010;38:65–75.

Han G, Liu C. Water geochemistry controlled by carbonate dissolution: a study of the river waters draining karst-dominated terrain, Guizhou Province, China. Chem Geol 2004;204:1-21.

Horowitz AJ, Meybeck M, Idlafkih Z, Biger E. Variations in trace element geochemistry in the Seine River Basin based on floodplain deposits and bed sediments. Hydrol Process 1999;13(9):1329–40.

Krishnaswami S, Singh S, Dalai T. Silicate weathering in the Himalaya: role in contributing to major ions and radiogenic Sr to the Bay of Bengal. In: Somayajulu BLK, editor. Ocean Science, Trends and Future Directions. New Delhi: Indian National Science Academy and Akademia International; 1999. p. 23–51.

Lerman A, Wu L, Mackenzie FT. CO_2 and H_2SO_4 consumption in weathering and material transport to the ocean, and their role in the global carbon balance. Mar Chem 2007;326:326–50.

Li SL, Calmels D, Han G, Gaillardet J, Liu CQ. Sulfuric acid as an agent of carbonate weathering constrained by $\delta^{13}C_{DIC}$: examples from Southwest China. Earth Planet Sci Lett 2008;270:189–99.

Meybeck M. Global analysis of river systems: from Earth system controls to Anthropocene syndromes. Philos Trans R Soc Lond B Biol Sci 2003;358:1935–55.

Meybeck M. Global geochemical weathering of surficial rocks estimated from river dissolved loads. Am J Sci 1987;287:401–28.

Meybeck M. Man and river interface: multiple impacts on water and particulates chemistry illustrated in the Seine River basin. Hydrobiologia 1998;373:1-20.

Millot R, Gaillardet J, Dupré B, Allégre CJ. The global control of silicate weathering rates and the coupling with physical erosion: new insights from rivers of the Canadian Shield. Earth Planet Sci Lett 2002;196:83–98.

Mortatti J, Probst JL. Silicate rock weathering and atmospheric/soil CO_2 uptake in the Amazon basin estimated from river water geochemistry: seasonal and spatial variations. Chem Geol 2003;197:177–96.

Oliva P, Viers J, Dupré B. Chemical weathering in granitic environments. Chem Geol 2003;202:225–56.

Pearl River Water Resources Committee (PRWRC). The Zhujiang Archive (in Chinese), vol. 1. Guangzhou, China: Guangdong Sci and Technol Press; 1991.

Picouet C, Dupré B, Orange D, Valladon M. Major and trace element geochemistry in the upper Niger river (Mali): physical and chemical weathering rates and CO_2 consumption. Chem Geol 2002;185:93-124.

Roy S, Gaillardet J, Allegre J. Geochemistry of dissolved and suspended loads of the Seine river, France: anthropogenic impact, carbonate and silicate weathering. Geochim Cosmochim Acta 1999;63:1277–92.

Sun HG, Han J, Zhang SR, Lu XX. The impacts of '05.6' extreme flood event on riverine carbon fluxes in Xijiang River. Chin Sci Bull 2007;52:805–12.

Tipper ET, Bickle MJ, Galy A, West AJ, Pomiès C, Chapman HJ. The short term climatic sensitivity of carbonate and silicate weathering fluxes: insight from seasonal variations in river chemistry. Geochim Cosmochim Acta 2006;70:2737–54.

Turner RE, Rabalais NN. Changes in Mississippi river water quality this century. Bioscience 1991;41:140–7.

Walker JCG, Hays PB, Kasting JFA. A negative feedback mechanism for the long term stabilisation of Earth's surface temperature. J Geophys Res 1981;86:9776–82.

Walling DE, Webb BW. Solutes in river systems. In: Trudgill ST, editor. Solute Processes. Chichester: Wiley; 1986. p. 251–327.

White AW, Blum AE. Effects of climate on chemical weathering in watersheds. Geochim Cosmochim Acta 1995;59:1729–47.

Xu JX. A study of anthropogenic seasonal rivers in China. Catena 2004;55:17–32.

Xu Z, Liu CQ. Chemical weathering in the upper reaches of Xijiang River draining the Yunnan-Guizhou Plateau, Southwest China. Chem Geol 2007;239:83–95.

Zhang S, Lu XX, Higgitt DL, Chen CA, Sun HG, Han J. Water chemistry of the Zhujiang (Pearl River): natural processes and anthropogenic influences. J Geophys Res 2007;112:1-17.

Zhang SR, Lu XX, Sun HG, Han J, Higgitt DL. Major ion chemistry and dissolved inorganic carbon cycling in a human-disturbed mountainous river (the Luodingjiang River) of the Zhujiang (Pearl River), China. Sci Total Environ 2009;407:2796–807.